Obrabotka metallov (tekhnologiya, oborudovanie, instrumenty) = Metal Working and Material Science. 2021 vol. 23 no. 1 pp. 68–78
ISSN: 1994-6309 (print) / 2541-819X (online)
DOI: 10.17212/1994-6309-2021-23.1-68-78

Obrabotka metallov -
Metal Working and Material Science

Journal homepage: http://journals.nstu.ru/obrabotka_metallov

Effect of mechanical activation of WC-based powder on the properties of sintered alloys

Ekaterina Abdulmenova [1, a, *], *Sergey Kulkov* [1, 2, b]

[1] Institute of Strength Physics and Materials Science of Siberian Branch of Russian Academy of Sciences, 2/4 pr. Akademicheskii, Tomsk, 634055, Russian Federation
[2] National Research Tomsk State University, 36 Lenin Avenue, Tomsk, 634050, Russian Federation

[a] https://orcid.org/0000-0002-9594-5706, Ekaterina.V.Abdulmenova@yandex.ru, [b] https://orcid.org/0000-0002-4635-6569, kulkov@ispms.ru.

ARTICLE INFO

Article history:
Received: 09 October 2020
Revised: 23 October 2020
Accepted: 14 December 2020
Available online: 15 March 2021

Keywords:
Wolfram carbide
Mechanical activation
Phase composition
Quasi-amorphous state
Coherently diffracting domain
Microdistortion
Lattice parameter
Porosity
Hardness

Funding
The results were obtained in the framework of the Integrated Project "Establishment of import-substituting high-tech full-cycle production of complex-shaped indexable carbide cutting inserts for priority industries" (Agreement No. 075-11-2019-036 dated November 27, 2019) implemented by the ISPMS SB RAS at the financial support of the Ministry of Education and Science of the Russian Federation as part of Decree of the Government of the Russian Federation No. 218 dated April 09, 2010.

Acknowledgements
The authors express their gratitude to the staff of the Laboratory of Physics of Nanostructured Functional Materials (LPNFM) for their help in preparing hard-alloy samples and help in preparation of sintered samples for further research.

ABSTRACT

Introduction. For the manufacture of wearproof tools and machine elements, the method of powder metallurgy is widely used. The preliminary high-

intensity mechanical activation of the powder is used to improve the structure and properties of the alloy obtained by the method of powder metallurgy. The mechanical activation can result in formation of nanostructures with subsequent amorphization of the material, can bring phase transformations, it can certainly affect the properties of the material. However, mechanical treatment does not always lead to a positive result. Therefore, the study of the effect of mechanical activation of WC-based powder on the properties of sintered alloys is important. **Purpose of the work:** to study the effect of high-intensity mechanical activation of WC-based powder on the structure and properties of sintered samples. The work investigates **alloys obtained** by the method of powder metallurgy, using mechanically activated powders for 10 to 300 seconds in a planetary ball mill. **Materials and methods.** The alloys are obtained by cold one-sided pressing followed by sintering at a temperature of 1400 °C in a vacuum furnace. Particle morphology of powder and structure of alloys is analyzed by scanning electron microscopy method. The metallographic analysis of the alloys is carried out by optical microscopy. Phase analysis and the parameters of the crystal structure are performed by X-ray diffraction. The hardness of the sintered samples is measured by hardness tester. **Results and its discussion**. It is shown that after sintering of powders alloys with WC and Co phases are formed. The lattice parameter of the WC-phase correlates well with values in literature. A second carbide phase, Co_3W_3C, is formed in the samples upon mechanical activation for more than 100 sec. The minimum porosity of sintered sample is 7.8 ± 1 % that corresponds of sample with preliminary mechanical treatment for 30 seconds. It is shown that the hardness depends on grain size, porosity and second carbide content. Thus, mechanical activation can be effective for increasing the physical and mechanical properties and inhibiting grain growth, but in this case, it is necessary to carry out mechanical processing in the mechanical treatment time range 60-100 sec.

For citation: Abdulmenova E.V., Kulkov S.N. Effect of mechanical activation of WC-based powder on the properties of sintered alloys. *Obrabotka metallov (tekhnologiya, oborudovanie, instrumenty) = Metal Working and Material Science*, 2021, vol. 23, no. 1, pp. 68–78. DOI:10.17212/1994-6309-2021-23.1-68-78. (In Russian).

*** Corresponding author**
Abdulmenova Ekaterina V., Postgraduate student
Institute of Strength Physics and Materials,
Science of Siberian Branch of Russian Academy of Sciences,
2/4 pr. Akademicheskii,
634055, Tomsk, Russian Federation
Tel.: 8 (3822) 286-988, **e-mail**: Ekaterina.V.Abdulmenova@ispms.ru

Introduction

Hard alloys based on tungsten carbide and cobalt (WC-Co) are widely used in the manufacture of cutting, drilling tools, wear-resistant parts due to their high hardness, strength, wear resistance, and good fracture toughness [1-3]. As a rule, by changing the structure of WC–Co hard alloys, for example, the composition of the alloy, the size of the carbide grains, the volume content of the binder component, it is possible to adjust the hardness, impact toughness, and strength [4]. The sintering process and the mechanical properties of such materials are significantly affected by the composition and microstructure, especially the grain size of the carbide phase [5], the content, and distribution of the cobalt binder [6-8]. At the same time, the presence of the η phase (W_3Co_3C) has a significant effect on the properties [3], and multi-stage sintering leads to a decrease in the grain size of the carbide phase, a decrease in the porosity of the sample. Paper [9] reports that using the method of rapid sintering with pulsed current activation can effectively suppress grain growth.

The use of nanocrystalline materials is known to improve physical and mechanical properties. Thus, paper [10] showed that when the particle size of TiC powder decreases from 380 to 60 nm, the hardness of sintered samples increases from ~ 28 (HV) to 32 GPa. It is possible to reduce the size of powder particles by using high-intensity mechanical processing in a planetary ball mill [11]. This method is relatively inexpensive and easy to implement [12]. In the process of high-intensity mechanical processing of powders, a state with a very small size of the coherent scattering region can be formed [13, 14], and [15, 16] showed that mechanical processing activates sintering with achieving a higher density and a smaller grain size [11, 17]. During such processing, the shape of the particles may also change, which, as a rule, will affect the physical and mechanical properties. For example, [18, 19] report that the lamellar shape of the particles allows increasing both the hardness of the material and viscosity.

It was shown in [20] that hard alloys with lamellar WC grains have a higher fracture toughness than hard WC-Co alloys with prismatic WC grains. However, it is known that mechanical processing does not always lead to a positive result, since such processing may cause contamination of powders, their oxidation, etc. [21, 22].

Thus, despite many research and practical publications devoted to the effect of high-intensity machining on the properties of alloys, the data on the effect of high-intensity machining of WC-Co powders on the morphology of particles, structure, phase composition, and physical and mechanical properties of sintered hard alloys are insufficient.

The purpose of this work is to study the effect of high-intensity mechanical activation of VK-8 powder on the structure and properties of powders and sintered samples. To achieve this purpose, the following **tasks were set: 1)** to study the morphology of the particles and their size by scanning electron microscopy before and after machining; **2)** to study the changes of the phase composition and parameters of the fine crystal structure by X-ray diffraction and X-ray structural analysis after machining; **3)** to study the microstructure of the sintered samples by optical and scanning electron microscopy; **4)** to study the changes of the phase composition and parameters of the fine crystal structure by X-ray diffraction and X-ray structural analysis of the sintered samples; **5)** to study the hardness of the sintered samples.

Research Methodology

The industrial powder of tungsten carbide of the VK-8 grade produced by Virial Ltd. was studied. The powder was processed in the planetary ball mill AGO-2 (Russia), the diameter of the steel balls was 0.7 cm, the ratio of powder to balls was 1:10, the rotation speed of the planetary disk was 1820 rpm, which provides an acceleration of 60g. The mechanical activation time was 10...300 seconds.

Pressing of the samples was carried out on a hydraulic press by cold one-sided pressing at a pressure of 200 MPa with pressure exposure of 15 s, sintering of the samples was carried out in a vacuum furnace SNVE 1.3.1/16 (Russia) according to the following mode:

a) heating from room temperature to 800 °C at a heating rate of 5 °C/min, followed by maintaining this temperature for 30 minutes;

b) heating from 800 °C to a sintering temperature of 1400 °C at a speed of 5 °C/min;

c) exposure at the sintering temperature for 60 minutes;

d) furnace cooling from the sintering temperature to room temperature.

The sintered samples were polished with diamond pastes of different dispersion. Metallographic analysis was performed using a Labomet-I microscope (Russia). The morphology of the powder particles and the microstructure of the sintered samples were studied by scanning electron microscopy (SEM) using a TESCAN VEGA3 SBH microscope.

To determine the structure and phase composition of the studied samples, the methods of X-ray diffraction and X-ray phase analysis were used. X-ray images were obtained using a DRON-3 diffractometer (Russia) with CuK_α radiation, the exposure to each point provides a statistical accuracy of at least 0.5 %. The parameters of the crystal lattice were determined using a program for X-ray diffraction calculations. The size of the coherent scattering region (SC R) was calculated using the Scherrer equation [23] for the first line of X-ray spectra, the microdisorsion value [24] was calculated using the Stock-Wilson formula for the last distinguishable line of X-ray spectra. For the calculation, the full width at half the maximum (FWHM) for each phase was determined. The diffraction profiles were approximated using the Lorentz function spectra.

The hardness of the sintered samples was measured on a Duramin 5 hardness tester (Denmark) at a load of 2 kg.

Results and discussion

Fig. 1 shows SEM images of powders in the initial state (*a*) and after mechanical activation for 30 s (*b*) and 300 s (*c*). In the initial state of the powder, there are agglomerates with a size of 350 ± 45 μm, which consist of small particles with a size of 7 μm. Mechanical activation leads to a decrease in the size of particles and agglomerates. Thus, the powder mechanically activated for 30 s consists of single agglomerates of 40 ± 10 μm with fine particles of 2 μm in its composition, and the powder after mechanical treatment for 300 s consists of agglomerates with an average size of 15 ± 5 μm containing fine particles of 1.4 μm. The shape of the particles does not change during mechanical activation and is close to spherical.

Figure 2 shows XRD patterns of powders at different times of mechanical activation. The reflections of WC and W_2C phases are seen on all XRD patterns. As the mechanical activation time increases, all the diffraction peaks of the phases widen. Additionally, the treatment for more than 100 s results in a broad component observed in the XRD patterns, which indicates the formation of an X-ray amorphous phase with a relative content up to 15 ± 5 % when treating the powder for 300 s. These results are consistent with [17], where an X-ray amorphous phase is also formed in WC-10Co-0.8VC-0.2Cr_3C_2 powder after treatment. The

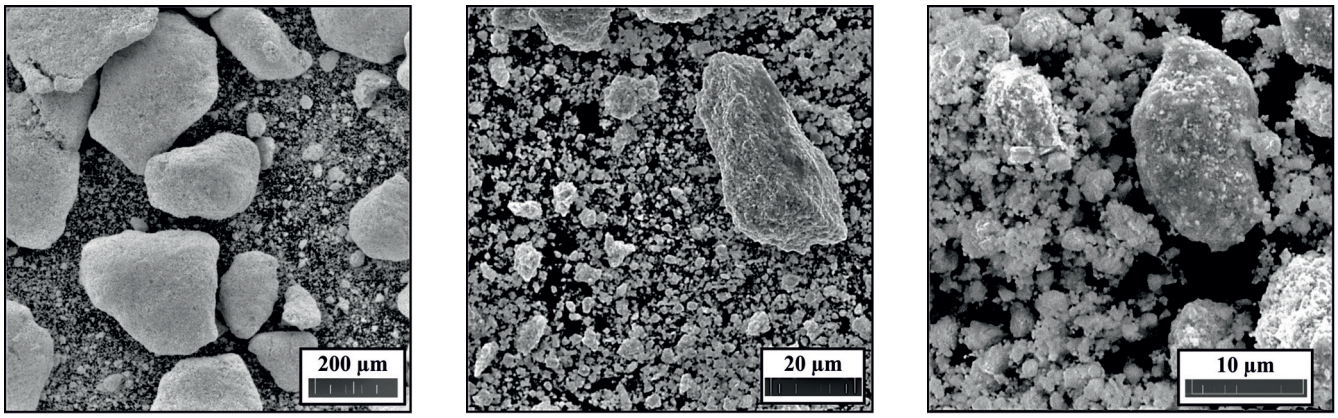

a *b* *c*

Fig. 1. SEM images of the powders:
the initial state (*a*); after ball milling for 30 (*b*) and 300 s (*c*)

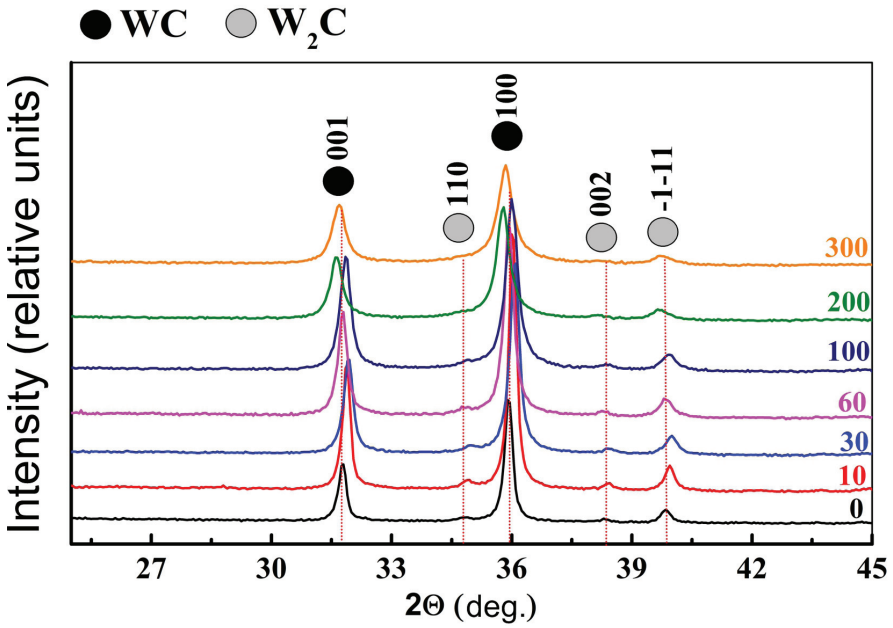

Fig. 2. XRD patterns of VK-8 powders in the initial state and after milling

relative content of W_2C of up to 60 seconds of mechanical activation does not change and is no more than 10±5%, and with a longer processing its content decreases to 3 ± 5 %. Perhaps the formation of the X-ray amorphous phase is due to the presence of the W_2C phase in the initial powders.

Figure 3 shows the dependence of the full width at half maximum of WC and X-ray amorphous phases on the time of mechanical activation. A significant change in the half-widths is seen to begin after 10 s of mechanical activation.

Fig. 4 shows the dependences of the CDD size (*a*) and microdistortion (*b*) calculated for the WC phase on the mechanical activation time. It can be seen that during the processing, the size of the CDD decreases from 47 ± 5 nm to 27 ± 5 nm, and the microdistortion increases from $1.1 \pm 0.03 \cdot 10^{-3}$ to $5.5 \pm 0.03 \cdot 10^{-3}$. In this case, 10 s is the time after which the size of the CDD and the lattice microdistortion begin to change.

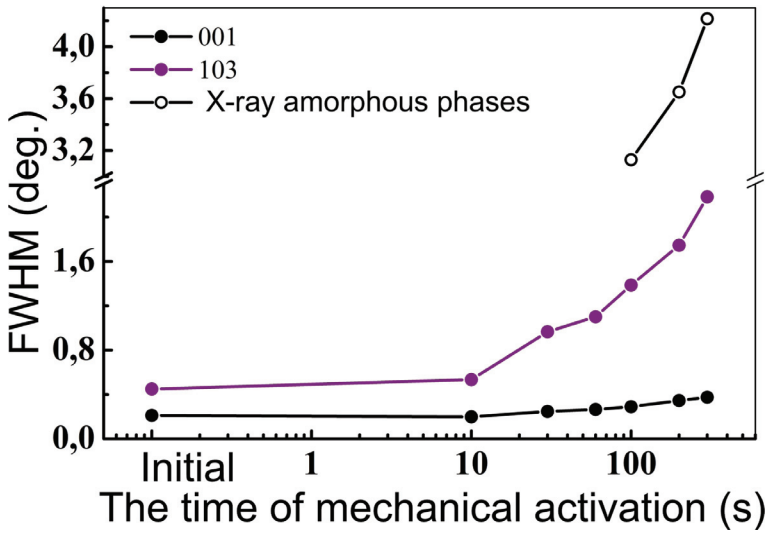

Fig. 3. The dependence of the full width at half maximum of WC and X-ray amorphous phases on the time of mechanical activation

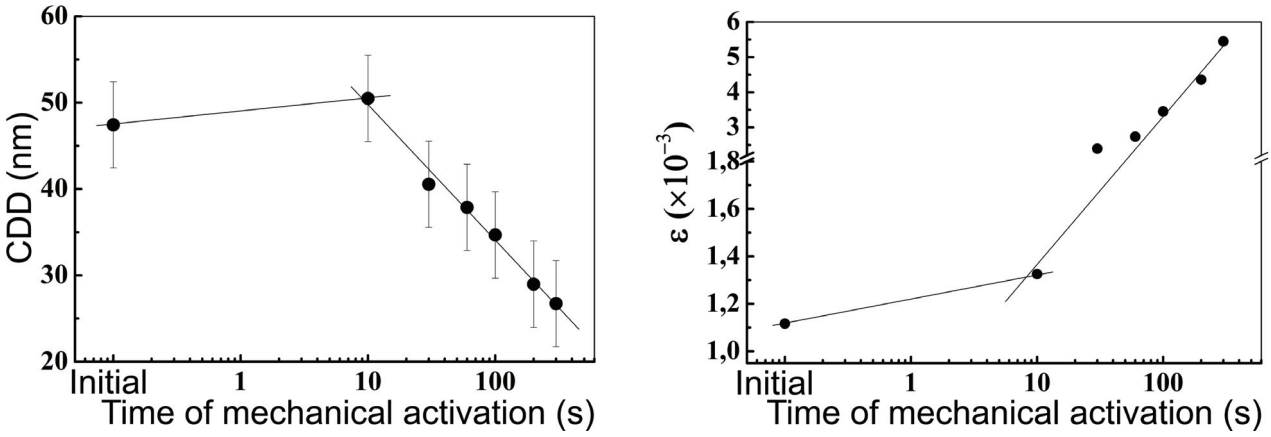

a *b*

Fig. 4. CDD size (*a*) and microdistortion (*b*) calculated for WC phase depending on the milling time

Figure 5 shows X-ray images of sintered samples. It can be seen that in all alloys there are WC and Co reflections, and in addition, the presence of the W_2C phase in the initial powder resulted in the formation of Co_3W_3C carbide, whose relative content does not exceed 16 ± 5 %.

Fig. 6 shows the dependence of the lattice parameter and the degree of the WC phase tetragonality on the time of the powder mechanical activation; they change insignificantly and are in good agreement with the literature data (ICDDPDF2 65-4539) [25].

Figure 7 shows SEM images of the structure of sintered samples and the grain size distribution. Pores are visible in the structures, the WC-phase grains have an irregular geometric shape (light areas), the W_2C phase (gray areas) is distributed mainly around the WC-phase grains. WC grains and the W_2C phase are uniformly distributed throughout the sintered sample. The average WC-phase grain size decreases with increasing machining time from 1.1 μm (σ = 0.6 μm) to 0.8 μm (σ = 0.3 μm) (at 300 s of powder machining).

Figure 8 shows the porosity of sintered samples depending on the time of the powders mechanical activation. It shows that at 10 s of processing the porosity is 11.6 ± 0.2 %, at 30 s of activation the porosity has a minimum value of 7.8 ± 1 % due to the destruction of agglomerates, and then begins to increase to 13.6 ± 1.5 % at longer processing.

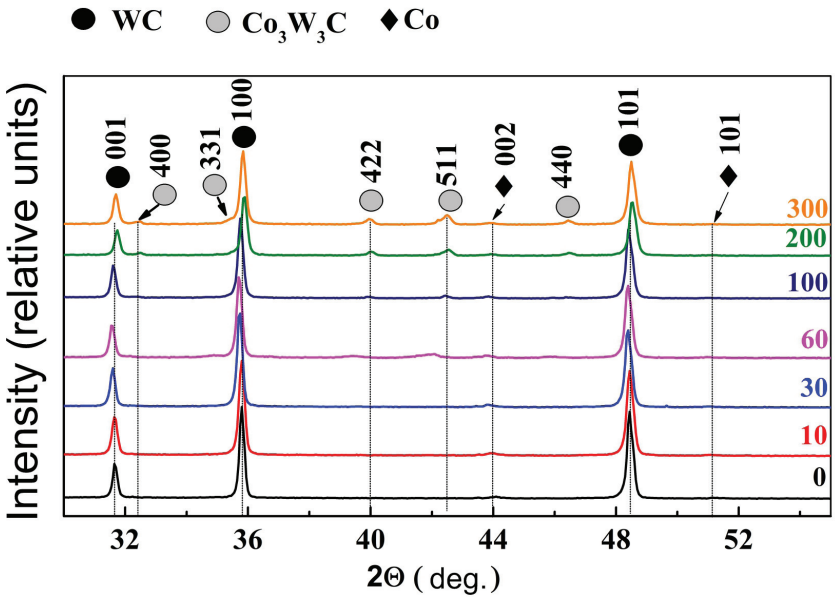

Fig. 5. XRD patterns of sintered samples depending on the milling time of powder

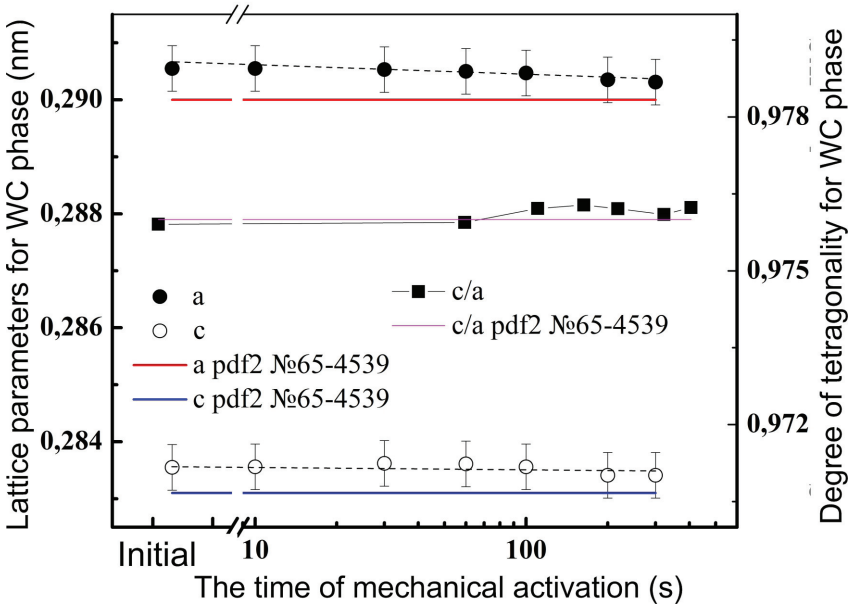

Fig. 6. Lattice parameters and degree of tetragonality for WC phase on the milling time of powder

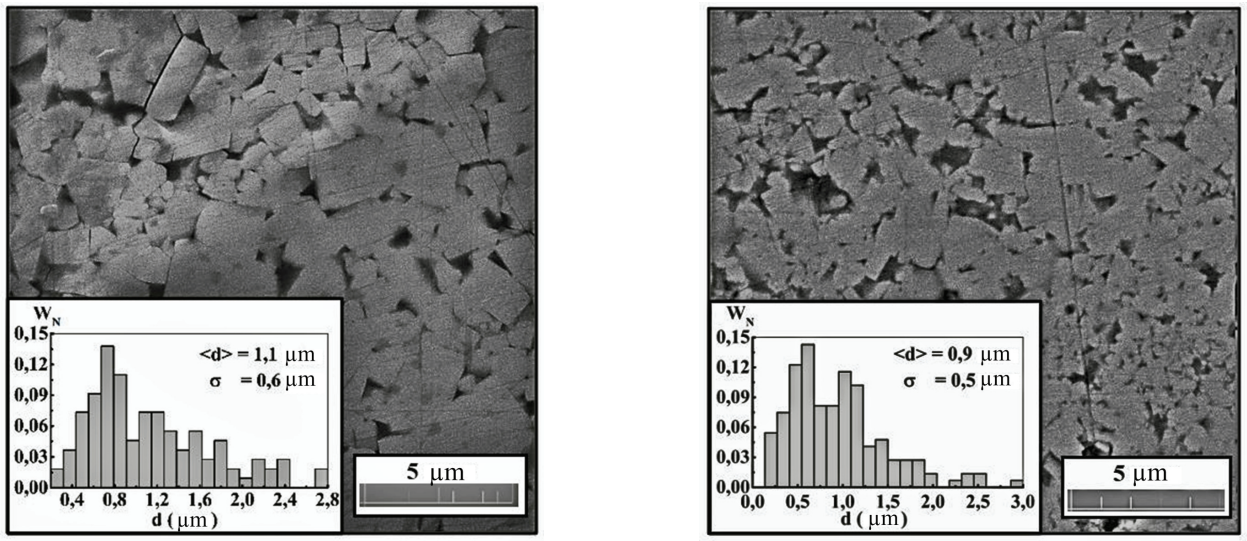

a *b*

Fig. 7. SEM images and grain size distribution: the initial state (*a*); after ball milling for 60 seconds (*b*)

Figure 9 shows the dependence of the hardness of sintered materials on the time of mechanical processing of powders, the literature data are also presented here [3]. The hardness of alloys is known depend on a number of parameters: grain size of the carbide phase, binder content, porosity, etc. [5, 26-29]. Therefore, it is difficult to make an unambiguous comparison with the data obtained; obviously, machining initially leads to a decrease in hardness, and then it increases again and at 60...100 s of processing *b* is close to the sintered material from untreated powder [3]. Apparently, the decrease in hardness in the sample at 10 s of treatment is due to the large grain size (1.2 μm σ = 0.6 μm) and significant porosity (11.6 ± 0.2 %). In a sample sintered from mechanically activated powder for 60 s the increase in hardness is, in contrast, associated with a decrease in both grain size (0.9 σ = 0.5 μm) and porosity (8.1 ± 0.5 %), however, with more intense mechanical activation hardness decreases slightly against a slight decrease in grain size and increased porosity.

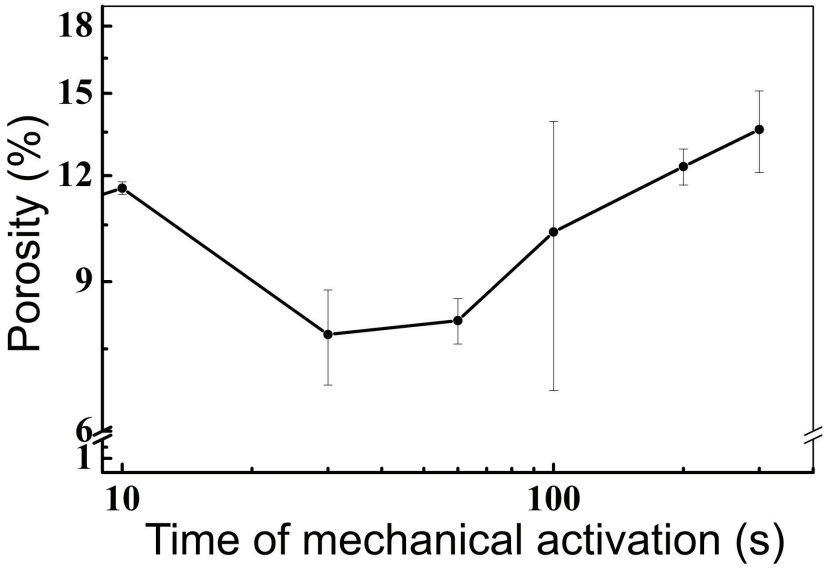

Fig. 8. Porosity of sintered samples depending on the milling time of powder

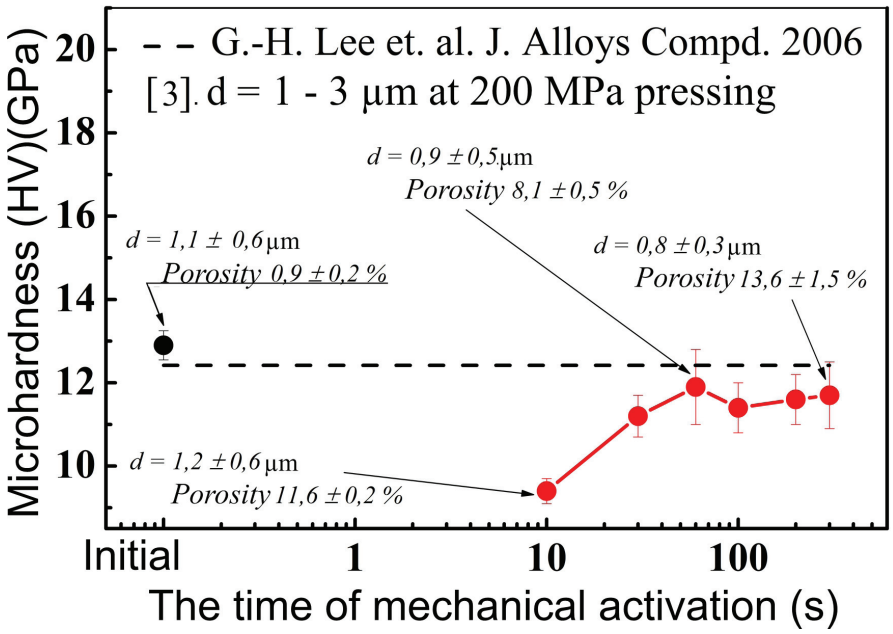

Fig. 9. Hardness of sintered samples depending on the milling time of powder

Conclusion

Studies have shown that mechanical activation of the powder leads to a decrease in the size of particles and agglomerates: as a result of the powder mechanical activation for 300 seconds, the size of aggregates decreased from 350 ± 45 to 15 ± 5 μm, and the average size of small particles decreased from 7 to 1.4 μm. It was found that when machining for more than 100 seconds, in addition to the crystalline WC- and W_2C-phases, an X-ray phase is formed, whose relative content does not exceed 15 ±5%. The crystal lattice parameter of the WC-phase during processing does not change and corresponds to the literature data. It is shown that the width of all peaks increases significantly after 10 s of machining, and when treated for 300 s, the size of the WC phase CDD decreases from 47 ± 5 nm to 27 ± 5 nm and the microdistortion increases from $1.1 \pm 0.03 \cdot 10^{-3}$ to $5.5 \pm 0.03 \cdot 10^{-3}$.

During sintering of powders at different mechanical activation times, WC- and Co-phases are formed, with the lattice parameter of the WC-phase corresponding to the tabulated value. The Co_3W_3C carbide phase is formed in the samples upon mechanical activation over 100 s. The average WC-phase grain size decreases from 1.1 μm (σ = 0.6 μm) to 0.8 (σ = 0.3 μm) with increasing machining time. The minimum porosity corresponds to 7.8 ± 1 % at 30 s of powder processing. It is shown that the hardness depends on both the time of mechanical activation and the grain size, porosity, and content of Co_3W_3C carbide.

Thus, mechanical activation can be effective for suppressing grain growth, but it should be carried out in the time interval of 60...100 s.

References

1. Ryu T., Sohn H.Y., Hwang K.S., Fang Z.Z. Plasma synthesis of tungsten carbide and cobalt nanocomposite powder. *Journal of Alloys and Compounds*, 2009, vol. 481 (1–2), pp. 274–277. DOI: 10.1016/j.jallcom.2009.03.134.

2. Shon I.-J., Kim B.-R., Doh J.-M., Yoon J.-K., Woo K.-D. Properties and rapid consolidation of ultra-hard tungsten carbide. *Journal of Alloys and Compounds*, 2010, vol. 489 (1), pp. L4–L8. DOI: 10.1016/j.jallcom.2009.09.040.

3. Lee G.-H., Kang S. Sintering of nano-sized WC-Co powders produced by a gas reduction-carburization process. *Journal of Alloys and Compounds*, 2006, vol. 419 (1–2), pp. 281–289. DOI: 10.1016/j.jallcom.2005.09.060.

4. Kim J.Y., Kang S.H. WC platelet formation via high-energy ball mill. *International Journal of Refractory Metals and Hard Materials*, 2014, vol. 47, pp. 108–112. DOI: 10.1016/J.IJRMHM.2014.06.024.

5. Kim B.K., Ha G.H., Lee D.W. Sintering and microstructure of nanophase WC/Co hardmetals. *Journal of Materials Processing Technology*, 1997, vol. 63, pp. 317–321. DOI: 10.1016/s0924-0136(96)02748-3.

6. Wang W., Lu Z., Zeng M., Zhu M. Achieving combination of high hardness and toughness for WC-8Co hardmetals by creating dual scale structured plate-like WC. *Ceramics International*, 2018, vol. 44 (3), pp. 2668–2675. DOI: 10.1016/j.ceramint.2017.10.190.

7. Stewart D.A., Shipway P.H., McCartney D.G. Microstructural evolution in thermally sprayed WC-Co coatings: comparison between nanocomposite and conventional starting powders. *Acta Materialia*, 2000, vol. 48 (7), pp. 1593–1604. DOI: 10.1016/s1359-6454(99)00440-1.

8. Fabijanić T.A., Alar Ž., Ćorić D. Influence of consolidation process and sintering temperature on microstructure and mechanical properties of near nano- and nanostructured WC-Co cemented carbides. *International Journal of Refractory Metals and Hard Materials*, 2016, vol. 54, pp. 82–89. DOI: 10.1016/j.ijrmhm.2015.07.017.

9. Kim H.-C., Shon I.-J., Yoon J.-K., Doh J.-M. Consolidation of ultrafine WC and WC-Co hard materials by pulsed current activated sintering and its mechanical properties. *International Journal of Refractory Metals and Hard Materials*, 2007, vol. 25 (1), pp. 46–52. DOI: 10.1016/j.ijrmhm.2005.11.004.

10. El-Eskandarany M.S. Structure and properties of nanocrystalline TiC full-density bulk alloy consolidated from mechanically reacted powders. *Journal of Alloys and Compounds*, 2000, vol. 305, pp. 225–238. DOI: 10.1016/s0925-8388(00)00692-7.

11. Raihanuzzaman R.M., Xie Z.H., Hong S.J. Powder refinement, consolidation and mechanical properties of cemented carbides – an overview. *Powder Technology*, 2014, vol. 261, pp. 1–13. DOI: 10.1016/j.powtec.2014.04.024.

12. Koch C.C. Synthesis of nanostructured materials by mechanical milling: problems and opportunities. *Nanostructured Materials*, 1997, vol. 9, pp. 13–22. DOI: 10.1016/s0965-9773(97)00014-7.

13. Vega L.E.R., Leiva D.R., Leal Neto R.M., Silva W.B., Silva R.A., Ishikawa T.T., Botta W.J. Mechanical activation of TiFe for hydrogen storage by cold rolling under inert atmosphere. *International Journal of Hydrogen Energy*, 2018, vol. 43 (5), pp. 2913–2918. DOI: 10.1016/j.ijhydene.2017.12.054.

14. Zaluski L., Tessier P., Ryan D.H., Doner C.B., Zaluska A., Ström-Olsen J.O., Trudeau M.L., Schulz R. Amorphous and nanocrystalline Fe-Ti prepared by ball-milling. *Journal of Materials Research*, 1993, vol. 8 (12), pp. 3059–3068. DOI: 10.1557/jmr.1993.3059.

15. Mushnikov N.V., Ermakov A.E., Uimin M.A. Kinetics of interaction of Mg-based mechanically activated alloys with hydrogen. *The Physics of Metals and Metallography*, 2006, vol. 102 (4), pp. 421–431. DOI: 10.1134/s0031918x06100097.

16. Stepanov A., Ivanov E., Konstanchuk I. Hydriding properties of mechanical alloys Mg-Ni. *Journal of the Less-Common Metals*, 1987, vol. 131, pp. 89–97. DOI: 10.1016/0022-5088(87)90504-2.

17. Sun J.F., Zhang F.M., Shen J. Characterizations of ball-milled nanocrystalline WC-Co composite powders and subsequently rapid hot pressing sintered cermets. *Materials Letters*, 2003, vol. 57, pp. 3140–3148. DOI: 10.1016/S0167-577X(03)00011-9.

18. Liu K., Wang Z.H., Yin Z.B., Cao L.Y., Yuan J.T. Effect of Co content on microstructure and mechanical properties of ultrafine grained WC-Co cemented carbide sintered by spark plasma sintering. *Ceramics International*, 2018, vol. 44, pp. 18711–18718. DOI: 10.1016/j.ceramint.2018.07.100.

19. Zhao Z.W. Microwave-assisted synthesis of vanadium and chromium carbides nanocomposite and its effect on properties of WC-8Co cemented carbides. *Scripta Materialia*, 2016, vol. 120, pp. 103–106. DOI: 10.1016/j.scriptamat.2016.04.024.

20. Kinoshita S., Saito T., Kobayashi M., Hayashi K. Microstructure and mechanical properties of new WC-Co base cemented carbide having highly oriented plate-like triangular prismatic WC grains. *Journal of the Japan Society of Powder and Powder Metallurgy*, 2000, vol. 47 (5), pp. 526–533. DOI: 10.2497/jjspm.47.526.

21. Nobuki T., Crivello J-C., Cuevas F. Fast synthesis of TiNi by mechanical alloying and its hydrogenation properties. *International Journal of Hydrogen Energy*, 2019, vol. 44, pp. 10770–10776. DOI: 10.1016/j.ijhydene.2019.02.203.

22. He M., Wang J.Y., He R.G., Yang H.L. Effect of cobalt content on the microstructure and mechanical properties of coarse grained WC-Co cemented carbides fabricated from chemically coated composite powder. *Journal of Alloys and Compounds*, 2018, vol. 766, pp. 556–563. DOI: 10.1016/j.jallcom.2018.06.366.

23. Scherrer P. Bestimmung der inneren Struktur und der Größe von Kolloidteilchen mittels Röntgenstrahlen. *Kolloidchemie Ein Lehrbuch*. Berlin, Heidelberg, Springer, 1912, pp. 387–409. DOI: 10.1007/978-3-662-33915-2_7.

24. Stokes A.R., Wilson A.J.C. The diffraction of X rays by distorted crystal aggregates. *Proceedings of the Physical Society*, 1944, vol. 56, pp. 174–181. DOI: 10.1088/0959-5309/56/3/303.

25. Bratanich T., Get'man O., Dobrovol'skii V., Kopylova L., Krapivka N., Permyakova T., Skorokhod V. Phase transformations and change in TiNi intermetallic compound structure during destructive hydrogenation and recombination. *Powder Metallurgy and Metal Ceramics*, 2006, vol. 45, pp. 582–587. DOI: 10.1007/s11106-006-0122-x.

26. Ban Z.G., Shaw L.L. Synthesis and processing of nanostructured WC-Co materials. *Journal of Materials Science*, 2002, vol. 37, pp. 3397–3403.

27. Berger S., Porat R., Rosen R. Nanocrystalline materials: a study of WC-based hard metals. *Progress in Materials Science*, 1997, vol. 42 (1–4), pp. 311–320. DOI: 10.1016/s0079-6425(97)00021-2.

28. Zhang F.L., Wang C.Y., Zhu M. Nanostructured WC/Co composite powder prepared by high energy ball milling. *Scripta Materialia*, 2003, vol. 49, pp. 1123–1128. DOI: 10.1016/j.scriptamat.2003.08.009.

29. Ding Q., Zhenga Y., Ke Z., Zhang G., Wu H., Xu X., Lu X., Zhu X. Effects of fine WC particle size on the microstructure and mechanical properties of WC-8Co cemented carbides with dual-scale and dual morphology WC grains. *International Journal of Refractory Metals and Hard Materials*, 2020, vol. 87, pp. 105166-1–105166-7. DOI: 10.1016/j.ijrmhm.2019.105166.

Conflicts of Interest

The authors declare no conflict of interest.